

UCSF

UC San Francisco Previously Published Works

Title

Correlative cryogenic tomography of cells using light and soft x-rays

Permalink

<https://escholarship.org/uc/item/8r45m7n5>

Authors

Smith, Elizabeth A
Cinquin, Bertrand P
Do, Myan
[et al.](#)

Publication Date

2014-08-01

DOI

10.1016/j.ultramic.2013.10.013

Peer reviewed

Published in final edited form as:

Ultramicroscopy. 2014 August ; 143: 33–40. doi:10.1016/j.ultramic.2013.10.013.

Correlative cryogenic tomography of cells using light and soft x-rays

Elizabeth A. Smith^{1,3}, Bertrand P. Cinquin^{1,3}, Myan Do^{1,3}, Gerry McDermott^{1,3}, Mark A. Le Gros^{1,2,3,*}, and Carolyn A. Larabell^{1,2,3,*}

¹Department of Anatomy, School of Medicine, University of California San Francisco, San Francisco, California

²Physical BioSciences Division, Lawrence Berkeley National Laboratory, Berkeley, California

³National Center for X-ray Tomography, Advanced Light Source, Berkeley, California

Abstract

Correlated imaging is the process of imaging a specimen with two complementary modalities, and then combining the two data sets to create a highly informative, composite view. A recent implementation of this concept has been the combination of soft x-ray tomography (SXT) with fluorescence cryogenic microscopy (FCM). SXT-FCM is used to visualize cells that are held in a near-native, cryo-preserved state. The resultant images are, therefore, highly representative of both the cellular architecture and molecular organization *in vivo*. SXT quantitatively visualizes the cell and sub-cellular structures; FCM images the spatial distribution of fluorescently labeled molecules. Here, we review the characteristics of SXT-FCM, and briefly discuss how this method compares with existing correlative imaging techniques. We also describe how the incorporation of a cryo-rotation stage into a cryogenic fluorescence microscope allows acquisition of fluorescence cryogenic tomography (FCT) data. FCT is optimally suited to correlation with SXT, since both techniques image the specimen in 3-D, potentially with similar, isotropic spatial resolution.

Keywords

Cell structure; imaging; molecular localization

1. Introduction

Microscopes for biological research come in all shapes and sizes, and range in complexity from simple light microscopes to highly sophisticated instruments that push the limits of existing technologies. Individually, all of these microscopes have one thing in common; they can only image specific cellular characteristics, and can't provide us with a highly complete

© 2013 Elsevier B.V. All rights reserved.

Corresponding Authors: Department of Anatomy, University of California San Francisco, 513 Parnassus Avenue, Box 0452, San Francisco, CA 94143-0452, CALarabell@ucsf.edu, MALegros@lbl.gov.

Publisher's Disclaimer: This is a PDF file of an unedited manuscript that has been accepted for publication. As a service to our customers we are providing this early version of the manuscript. The manuscript will undergo copyediting, typesetting, and review of the resulting proof before it is published in its final citable form. Please note that during the production process errors may be discovered which could affect the content, and all legal disclaimers that apply to the journal pertain.

view of both cell ultrastructure and molecular organization. As a result, it is rare that data from any one modality can answer the types of question posed in cell biology. To overcome this shortfall much effort has been directed towards the development of correlative microscopy, where the specimen is imaged by two complementary modalities and the data combined to generate a significantly more comprehensive view of the specimen. In the case of correlated light- and electron microscopy (CLEM) this approach has proven to be very effective [1-10]. CLEM is a highly informative combination of modalities, and remains the focus of significant ongoing development. That said, there is still a pressing need to develop new correlative techniques, in particular using techniques that combine modalities with different image contrast mechanisms to electron microscopy [11-18]. Here we outline recent progress in combining soft x-ray tomography (SXT) with high-numerical aperture, fluorescence cryogenic microscopy (FCM) to create a new correlative method. SXT is used to quantitatively image cells and their sub-cellular structures [11, 19]. FCM is used to generate molecular localization data, and/or confirm the identity of structures and organelles in SXT reconstructions [11, 20-23]. The combination of these two modalities permits an enormous array of cellular features to be identified and quantified. In short, the output of correlated SXT-FCM is significantly more than the sum of the component modalities. Below we will first briefly describe alternative correlative microscopies to SXT-FCM, in particular CLEM, to highlight the unique niche filled by this new correlated modality. We will then describe the important characteristics of both SXT and FCM, particularly those characteristics that make them well suited to correlated studies. Finally, since correlated SXT-FCM is a relatively new technique, we will close by discussing the near term future prospects, the most exciting of which is equipping the FCM with a rotation stage that enables acquisition of fluorescence cryo tomographic (FCT) data. The application of tomographic methods to FCM greatly reduces anisotropy in the fluorescence signal (in standard light microscopy approaches the spatial resolution is significantly better in x and y than it is in z, i.e. the axis along the illumination light path through the specimen) and allows molecules to be localized with much greater precision. Since FCT and SXT are both 3-D techniques, and potentially produce data with similar spatial accuracy and precision, these two types of reconstruction can be confidently correlated.

As with the individual modalities, the combination of SXT-FCT can be applied to a wide range of cell types, ranging from small bacteria, through to large eukaryotic cells. Any cell that falls within the size constraints placed by SXT is suitable (i.e. a maximum thickness of 15 μ m). As will be described below the specimen mounting system used determines the overall characteristics of the specimens that can be imaged [17]. Large adherent cells are imaged on TEM style grids [14]. Whereas, cells grown in suspension – provided they meet the size criteria above – are best imaged mounted in thin-walled glass capillary tubes [24]. The fluorescent signal can be derived from any of the labeling methods commonly used in cell biology (genetically encoded fluorescent proteins or small molecule stains). Consequently, SXT-FCT can meet most imaging needs in cell biology, whether it is imaging the effect of candidate drug molecules on pathogenic microbes, or determining the structural consequence of genetic mutations or environmental factors on human cells.

2. Comparison of SXT-FCM with other correlative techniques

In CLEM the cell ultrastructure is visualized by electron microscopy and molecular localization using fluorescence. Of course, molecules can also be localized directly in an electron micrograph if they have been labeled with electron-dense tags. However, given the enormous body of cell biology research that has been carried out using FP labeled molecules [25-27] it is highly advantageous to combine ultrastructural imaging with fluorescence data [28]. Adopting this approach has presented a number of challenges, many of which have been successfully overcome in cases where the specimen has been chemically fixed [10]. However, in cryo-EM obtaining fluorescence data from a cryopreserved specimen has proven more difficult. To date, the fluorescence microscopes used in cryo-CLEM studies have all employed low numerical aperture (NA) air lenses (that is to say, an NA of 1.0 or lower) [7-9, 29-31]. Lenses such as these are not well matched to the refractive index (RI) of the specimen. The mismatch in the RI of air compared to the specimen leads to blurring and a reduction in the precision with which molecules can be localized [20]. The major advantage of FCM is the use of lenses that are coupled to the specimen by an index-matched immersion fluid (such as propane, RI 1.32). This coupling greatly improves image quality, and allows the use of higher numerical aperture lenses [20, 21, 23].

3. Specimen mounting and preservation for correlative SXT and FCM

As with any correlated imaging experiment, the SXT-FCM specimen mounting system must be robust, easy to handle, and not interfere with image acquisition in either microscope. Currently, two different systems predominate; one based on TEM style grids [13, 32, 33], the other, thin-walled capillary tubes [17, 24, 34, 35]. Naturally, each has inherent advantages and disadvantages. TEM grids can be used to mount large, adherent cells, and even allow cells to be cultured *in situ* on the grid. Whilst this is a very positive advantage it also places restrictions on the rotation of the specimen to a maximum of $\pm 70^\circ$ [32]. As the grid is tilted the specimen becomes thicker with respect to the illumination axis, and therefore more strongly absorbing, eventually reaching a point where there is insufficient transmission of the specimen illumination [32]. Systematically missing data associated with limited tilt tomography negatively impacts tomographic reconstructions and leads to obvious artifacts. On the other hand, when the specimen is mounted in a thin-walled glass capillary it can be viewed from any perspective without an apparent increase in thickness. The disadvantage, however, is that the capillary diameter is restricted to $\sim 15\mu\text{m}$ (i.e. the maximum thickness of specimen that can be imaged by SXT). In summary, the decision between which specimen mounting system to use comes down to the size of specimen being imaged, for cells up to $15\mu\text{m}$ in size capillaries are the optimal choice (completeness of data), for large, extended specimens a TEM grid is the only choice if the specimen is to be imaged intact (capillaries can be used to mount large cells if they are resuspended, or even tissue sections if they are sectioned using a microtome, or de-bulked using techniques such as ion milling). The correlated imaging system developed at the National Center for X-ray Tomography (ncxt.lbl.gov) has focused primarily on the use of glass capillaries. The walls of these capillaries are 250-400 nm thick, this is thin enough that both x-ray and light microscopy can be performed with minimal degradation in the signal [36]. When mounted in a suitable rotation stage, a capillary can be rotated to any arbitrary angle for tomographic

data acquisition [22-24]. The importance of this factor can't be understated when the goal is collection of tomographic data since the reconstruction algorithms are highly sensitive to missing data (as occurs when rotation of the specimen is limited) [37].

In all tomographic methods the specimen is imaged a number of times [38]. Repeated exposure of the specimen to harsh illumination has, of course, the potential to cause damage, particularly in x-ray imaging where damage is cumulative as a function of received dose [39-41]. Preserving the specimen, either chemically or cryogenically, can mitigate damage during data acquisition, at least to the point it is not visible in the image [11, 36, 42]. Cryopreservation is generally accepted to be the preferred method, since this has been shown to retain the fine structural details and *in vivo* molecular organization much more effectively than chemical fixation [43-45]. Consequently, cryopreservation is the preferred fixation method for correlated SXT-FCM [23, 32]. In addition, cryopreservation has the added benefit of increasing the working lifetime of the fluorescence labels, typically by a factor of 30 or greater [20, 46]. This increase in working lifetime makes fluorescence tomography viable, since the fluorescence signal remains largely constant throughout the process of image acquisition. Again, this is an enormously significant factor, since loss of fluorescence in the later stages of data collection would impart significant noise into the tomographic reconstruction.

4. High numerical aperture fluorescence cryo-microscopy

Fluorescence microscopy (FM) is one of the most commonly performed imaging techniques in cell biology, and as such needs little further discussion beyond acknowledging the power of genetically encoded probes, and the ability to label almost any molecule in a cell with a fluorescent tag of a chosen color [26]. This technology has been revolutionary, and has made an enormous impact in the scientific literature. Therefore, FM is an obvious partner to use in conjunction with a modality that visualizes cell structure.

Early work aimed at correlating SXT and FM data relied on room-temperature confocal fluorescence microscopy of chemically fixed, dehydrated specimens [47]. Whilst interesting and significant in the field, this work fell short of the mark in terms of being informative. For example, the cells were undoubtedly far from representative of their *in vivo* state by virtue of the fixation method used and the fact that the cells were dehydrated. However, this work made the goal for future developments patently clear – to create a system that allows specimens to be imaged in a near-native state, and with fluorescence imaging that has the best possible fidelity. This meant collecting FM data from cryopreserved, rather than chemically fixed, dehydrated specimens, and using cryogenic immersion fluid, rather than air, to couple the lens to the specimen [22]. Since no commercial microscopes were available that met these criteria, NCXT staff built a custom designed instrument [20]. The first generation FCM fulfilled the goals of allowing cryopreserved specimens to be imaged in refractive index matched fluids and therefore permitted the use of high numerical-aperture lenses [20].

The FCM operates 10 - 20° K above liquid nitrogen temperature and uses liquid propane (refractive index = 1.32) or iso-pentane (refractive index = 1.35) as immersion fluid. The

design of this microscope is shown in Fig. 1. The maximum resolution achieved by conventional fluorescence microscopy is inversely proportional to the numerical aperture (NA) of the microscope. The presence of the immersion fluid increases the NA of the microscope and therefore also increases the maximum-attainable spatial resolution. In addition, using refractive index-matched cryogenic immersion fluid increases the light collection efficiency of the microscope by lowering the amount of light that is reflected at the boundaries between materials with different refractive indices [20]. Taken together, the design strategy of the FCM enables high-quality fluorescence imaging with spatial resolution and collection efficiency that is comparable to that achieved using conventional, high NA room temperature microscopes. To further boost performance, the high NA cryofluorescence microscope was fitted with a spinning disk confocal unit [17], which reduces contributions from scatter and fluorescence that arise from out-of-focus regions of the specimen.

FCM has many advantages over imaging at room temperature. The fluorescence emission spectra of many fluorophores are narrower at cryogenic temperature compared with room temperature. Narrower emission spectra permit the use of emission filters with a smaller bandwidth without compromising light collection efficiency or increasing cross talk [46]. The working lifetime of fluorescent proteins is extended by a factor of 30 or more at cryogenic temperatures [46]. This allows the collection of data with greatly improved signal-to-noise ratio before the fluorescent signal is destroyed (i.e. irreversibly photo-bleached) compared with room temperature imaging. Brownian motion and dynamic cell processes are essentially stopped in a vitrified specimen at cryogenic temperatures [45]. This permits long or repeated exposures during imaging so that weak signals can be detected. Photo-bleaching that does occur is less sensitive to its local chemical environment so the fluorescence intensity in a local environment reflects the local concentration of fluorophore more accurately than is possible at room temperature. Tomographic data collection, in which the specimen is imaged successively from many different angles, can also be performed. Reconstructed fluorescence tomography data can achieve isotropic spatial resolution instead of the approximately 3-fold reduction in resolution that usually occurs along the optical (z) axis [48]. Now that we have outlined SXT and FCM, we will discuss how the data can be correlated.

5. Soft X-ray tomography (SXT)

Prior to describing SXT it is important to differentiate between SXT and diffraction imaging microscopy (DIM), since these conceptually different forms of x-ray imaging are commonly confused. In DIM, the physical lenses used in a conventional microscope are replaced by computer algorithms, and rather than collecting real-space projection images, the camera records reciprocal space diffraction from the specimen [49]. As a consequence, unlike in conventional microscopy where a recognizable image of the specimen is recorded on the detector, in DIM the collected images are arrangements of intensities that bear no resemblance to the specimen whatsoever. In concept, DIM imaging is analogous to x-ray crystallography, except that the specimen is composed of a single, unique object (i.e. an isolated cell) rather than of multiple copies in the form of a crystal. The diffraction pattern produced by the specimen can be inverted by phase retrieval methods similar to those used

in crystallography and astronomy (this computational process is analogous to the work performed by a lens). In principle, DIM could be used to image a cell with near atomic spatial resolution. In practice, however, it has proven difficult to achieve anywhere close to this resolution. In the first example of using DIM to examine biological specimens, Miao and colleagues reported a 35 nm spatial resolution reconstruction of a bacterial cell [50]. Later reports used DIM to produce images of yeast and other cells but these images contained remarkably little structural information compared with images obtained by other techniques, such as SXT or electron tomography [49, 51, 52]. Consequently, significant technical difficulties must be overcome before imaging a cell using DIM can be considered routine practice.

Soft x-ray microscopes follow the same optical design principles as a simple bright-field light microscope (see Fig. 2 for a schematic diagram of XM-2, a soft x-ray microscope located at the Advanced Light Source, Berkeley, and Text box 1 for a summary of the technique). A condenser lens focuses the illuminating light onto the specimen. The transmitted illumination then passes through an objective lens on its way to a detector, typically a charge coupled device (CCD). Unlike a light microscope, a soft x-ray instrument cannot be operated with glass lenses, as thick glass lenses would absorb the majority of the illuminating photons [53]. Instead, soft x-ray microscopes are equipped with Fresnel Zone plates, which are nanofabricated diffractive optics, comprised of a series of concentric rings [54, 55]. The rings alternate between being opaque and transmissive to soft x-rays [53]. The spatial resolution with which these instruments can image is largely determined by the width of the outermost ring [53, 56, 57]. Currently, the resolution is in the range of 35 to 50 nm (half-pitch). However, zone plate optics can now be manufactured to have an outer zone width of better than 15 nm [54].

In transmission soft x-ray microscopy, the image contrast is derived from the attenuation of the illumination by the specimen {Weiss, 2001 #22; Schneider, 2003 #16; Schneider, #1393; Schmahl, 2007 #207, Meyer-Ilse, 2001 #9; Larabell, 2004 #1394}. Typically for biological imaging the specimen is illuminated with photons in the so-called 'water window,' that is the energy range (2.3 - 4.4 nm, 0.28 - 0.53 keV) between the absorption edges of oxygen (water) and carbon (biomolecules). In this regime, water attenuates soft x-rays an order of magnitude less than carbon- and nitrogen-containing entities, such as proteins or lipids [53]. This attenuation follows the Beer-Lambert law, and is therefore quantitative and a function of chemical species and thickness. In a soft x-ray micrograph of a cell, regions that are densely packed with proteins or lipid will strongly attenuate the illumination whereas highly solvated regions will attenuate weakly [42]. This phenomenon gives rise to the excellent contrast seen in this form of cell imaging and allows regions of the cell to be readily segmented into organelles with subsequent delineation of the organelle substructure [21, 23]. In practice, this requires 3-dimensional information. We will explain below how 3-dimensional reconstructions of a cell can be calculated from a number of 2-dimensional projection images.

6. Data Collection

Fluorescence data is collected first from the specimen since illumination with soft x-rays is liable to irreversibly quench the fluorescence signal. Through-focus data stacks, in which a series of images is taken while the specimen is moved stepwise along the optical axis of the microscope, are collected. Using standard lasers and a CCD detector typical exposure times for each image are ~100 ms. If tomographic fluorescence data are required, this process is repeated at a number of different angles around a central rotation axis. The specimen is then cryo-transferred to and located in the soft x-ray microscope. This workflow is shown in Fig. 3. After cryo-transfer to the x-ray microscope, the same specimen within the capillary tube is quickly and easily located in the x-ray microscope by measuring its distance from the capillary tip. This is possible because the capillaries are mounted to stages that are controlled by motorized micromanipulators that move with submicron accuracy. In cases where the capillary is crowded with cells, bright-field and/or fluorescence images taken with the cryo-light microscope can aid in identifying a particular specimen. Projection data is collected from the x-ray microscope while the specimen is rotated around an axis perpendicular to the optical axis of the microscope. A typical x-ray dataset has 180 projections with 150 ms exposures per projection. The soft x-ray projection data is aligned and used to calculate a three-dimensional reconstruction of the specimen.

7. Building a 3D reconstruction from 2D imaging data

Microscopes can only produce two-dimensional projection images of the specimen [37]. In a soft x-ray microscope projection image of a cell, the sub-cellular structures are superimposed on top of each other, making interpretation difficult, if not impossible. Consequently, in most instances a cell ultrastructure must be imaged in 3D. Collecting projection images at angular increments around a rotation axis and calculating a 3D reconstruction of the specimen easily achieve this [38]. Tomography is a very well-established methodology, and used extensively in hospitals and clinics throughout the world in the form of CT (computed tomography) scanners. SXT operates on similar concepts, but at significantly higher spatial resolution (50 nm or better). In SXT, the x-ray source and detector remain fixed and the specimen is rotated inside the microscope.

Similar tomographic reconstruction algorithms can be applied to FCM data if fluorescence images are acquired at a number of different angles around a rotation axis. In a single 2D fluorescence image from the FCM, the aberrations in the lens system cause the fluorescence signal from a point source to appear elongated along one axis (i.e. a point of light is cigar-shaped in the image). Imaging the signal from multiple perspectives eliminates this type of effect, and the point of light appears spherical (Smith et al, 2013 -submitted). Similar results would be obtained if the specimen were imaged at room temperature [48]. However, at room temperature, damage to the fluorescent-labels (i.e. photon induced bleaching) would destroy the fluorescence signal and preclude the collection of large numbers of fluorescence images from the specimen, plus the specimen would be susceptible to movement if it were not cryopreserved.

8. Aligning and correlating SXT and FCT reconstructions

In order for the fluorescence and x-ray datasets to truly provide complementary, useful information, they must be aligned to each other with high accuracy. Feature-based alignment strategies, such as mutual information algorithms, may be applicable to align large, general features such as the plasma membrane of a cell. However, the best alignment strategy is completely objective, robust, and is done with high accuracy. Ideally, errors in aligning the two datasets will be considerably less than the resolution of the lower-resolution modality. An effective strategy is to use correlative fiducial markers that are visible in both the fluorescence data and the SXT reconstructions[32]. For correlated SXT-CFT “joint fiducial” markers can be stably conjugated to the outside of the capillary specimen tube. The fluorescence spectra of these markers are spectrally distinct, and collected simultaneously with, fluorescence from the specimen. For this purpose, fluorescent polystyrene microspheres or surface-functionalized fluorescent gold nanoparticles can be used. The practical application of this approach is discussed in greater detail in [17, 18, 32] and an example shown in Fig. 4.

9. Future of Correlative SXT-FCM

SXT-FCM is a recent combination of techniques. As such, there remains much scope for enhancement and extension. For example, the optical or imaging systems can be made significantly better in both modalities. In the case of FCM, lenses can be designed from the ground up to have optimal characteristics in a cryogenic environment. The choice of immersion fluid can also be matched more closely to both the specimen and the optical system of the microscope. Improvements to the optical system also open up the possibility of using ‘super resolution’ techniques to improve the precision with which molecules can be localized. Of the various methods for achieving this, the obvious first choice would be ‘structured illumination’ [58, 59] because it does not rely on particular probe characteristics, such as ‘blinking’, which may be affected by imaging at low temperature. Overall, the FCM design is straightforward and built from relatively inexpensive components. Other groups can easily build their own FCM, either for use as a stand-alone instrument – to take advantage of the increase in fluorescence working life – or for use in tandem with other modalities, in particular electron microscopy.

For SXT, the optical elements in a soft x-ray microscope used to collect data can be modified to allow higher spatial resolution data [54]. This can be achieved simply by employing the latest generation of high-resolution zone plates. There is no inherent difficulty in collecting data with these lenses. However, as the spatial resolution of the microscope increases, the depth of field decreases, to the point that it is less than the thickness of the specimen. This problem is exacerbated with increasing numerical aperture optics. This calls for the application of modified data acquisition strategies, for example a combination of deconvolution with tomography.

In terms of making the technique more widely used and easier to access, Hertz and co-workers have made significant progress towards developing a laboratory, or “table-top” soft x-ray microscope that would not rely on synchrotron radiation as an x-ray source [60]. Their

microscope focuses high-intensity laser pulses onto a liquid Nitrogen jet, which produces a 2.48 nm water-window x-ray source. This source is imaged onto the specimen using a normal incidence multilayer condenser/monochromator and a Fresnel objective zone plate focuses the transmitted light onto a CCD. Imaging of test patterns has shown that these table-top soft x-ray microscopes compare favorably with synchrotron-based microscopes [60]. Tomographic imaging of frozen hydrated cells is also possible within a modified TEM cryo/tilt sample chamber. The major drawback with their current tabletop system is that the low brightness of the source requires exposure times 20-50 times greater than similar microscopes at the synchrotron source. In addition to minimizing specimen throughput, the need for long exposures makes high demands on instrument stability. Tomographic techniques are particularly sensitive to movement of the specimen during data collection because this results in artifacts in the final reconstructions. Hertz and co-workers have outlined a strategy to reduce the exposure time a factor of 10 or more - if this is achieved successfully, tabletop SXT could be accessible to a much wider community.

10. Conclusions

Correlative SXT and FCM is a very welcome new addition to the cell biologist's imaging toolkit. This combination of modalities allows molecular localization data to be viewed in the context of high-resolution tomographic reconstructions of cells, or even tissue sections. As with all modalities or combinations of modalities, this development fills a particular niche in terms of information content. SXT-FCM is ideally suited to determining the structural consequences of events at the molecular scale. In particular, linking phenotype to the location of particular molecules will enable answering questions such as “where in the cell is a specific molecule sequestered?” or “what are the consequences of experimental manipulations on sub-cellular organization?” Correlative microscopy is an expanding area in cell biology and will likely remain so for the foreseeable future. Therefore, it is important that we have access to microscopes with as many different contrast mechanisms as possible. These new modalities can easily function in tandem with other modalities, for example electron microscopy, presenting opportunities to develop new multi-modal tools for cellular imaging.

Acknowledgments

This work was supported by the US Department of Energy, Office of Biological and Environmental Research (DE-AC02-05CH11231), the National Center for Research Resources of the National Institutes of Health (P41RR019664) and the National Institutes of General Medicine of the National Institutes of Health (GM63948), and the Gordon and Betty Moore Foundation.

References

1. Martone ME, Deerinck TJ, Yamada N, Bushong E, Ellisman MH. Correlated 3D light and electron microscopy: Use of high voltage electron microscopy and electron tomography for imaging large biological structures. *J Histotechnol.* 2000; 23:261–270.
2. Takizawa T, Robinson JM. FluoroNanogold is a bifunctional immunoprobe for correlative fluorescence and electron microscopy. *J Histochem Cytochem.* 2000; 48:481–486. [PubMed: 10727289]

3. Giepmans BN, Deerinck TJ, Smarr BL, Jones YZ, Ellisman MH. Correlated light and electron microscopic imaging of multiple endogenous proteins using Quantum dots. *Nat Methods*. 2005; 2:743–749. [PubMed: 16179920]
4. Grabenbauer M, Geerts WJ, Fernandez-Rodriguez J. Correlative microscopy and electron tomography of GFP through photooxidation. *Nat Methods*. 2005; 2:857–862. [PubMed: 16278657]
5. Sartori A, Gatz R, Beck F, Kossel A, Leis A, Baumeister W, Plitzko JM. Correlation microscopy: Bridging the gap between light- and cryo-electron microscopy. *Microsc Microanal*. 2005; 11:16–17.
6. Plitzko JM, Rigort A, Leis A. Correlative cryo-light microscopy and cryo-electron tomography: from cellular territories to molecular landscapes. *Curr Opin Biotechnol*. 2009; 20:83–89. [PubMed: 19345086]
7. Rigort A, Bauerlein FJ, Leis A, Gruska M, Hoffmann C, Laugks T, Bohm U, Eibauer M, Gnaegi H, Baumeister W, Plitzko JM. Micromachining tools and correlative approaches for cellular cryo-electron tomography. *J Struct Biol*. 2010; 172:169–179. [PubMed: 20178848]
8. Caplan J, Niethammer M, Taylor RM 2nd, Czymmek KJ. The power of correlative microscopy: multi-modal, multi-scale, multi-dimensional. *Curr Opin Struct Biol*. 2011; 21:686–693. [PubMed: 21782417]
9. Ellisman MH, Deerinck TJ, Shu X, Sosinsky GE. Picking faces out of a crowd: genetic labels for identification of proteins in correlated light and electron microscopy imaging. *Methods Cell Biol*. 2012; 111:139–155. [PubMed: 22857927]
10. Kopek BG, Shtengel G, Xu CS, Clayton DA, Hess HF. Correlative 3D superresolution fluorescence and electron microscopy reveal the relationship of mitochondrial nucleoids to membranes. *Proc Natl Acad Sci U S A*. 2012; 109:6136–6141. [PubMed: 22474357]
11. Larabell CA, Nugent KA. Imaging cellular architecture with X-rays. *Curr Opin Struct Biol*. 2010; 20:623–631. [PubMed: 20869868]
12. Hagen C, Guttman P, Klupp B, Werner S, Rehbein S, Mettenleiter TC, Schneider G, Grunewald K. Correlative VIS-fluorescence and soft X-ray cryomicroscopy/tomography of adherent cells. *J Struct Biol*. 2012; 177:193–201. [PubMed: 22210307]
13. Muller WG, Heymann JB, Nagashima K, Guttman P, Werner S, Rehbein S, Schneider G, McNally JG. Towards an atlas of mammalian cell ultrastructure by cryo soft X-ray tomography. *J Struct Biol*. 2012; 177:179–192. [PubMed: 22155291]
14. Schneider G, Guttman P, Rehbein S, Werner S, Follath R. Cryo X-ray microscope with flat sample geometry for correlative fluorescence and nanoscale tomographic imaging. *J Struct Biol*. 2012; 177:212–223. [PubMed: 22273540]
15. Chichon FJ, Rodriguez MJ, Pereiro E, Chiappi M, Perdiguero B, Guttman P, Werner S, Rehbein S, Schneider G, Esteban M, Carrascosa JL. Cryo X-ray nanotomography of vaccinia virus infected cells. *J Struct Biol*. 2012; 177:202–211. [PubMed: 22178221]
16. Luger K, Dechassa ML, Tremethick DJ. New insights into nucleosome and chromatin structure: an ordered state or a disordered affair? *Nat Rev Mol Cell Biol*. 2012; 13:436–447. [PubMed: 22722606]
17. Cinquin BP, Do M, McDermott G, Walters AD, Myllys M, Smith EA, Cohen-Fix O, Le Gros MA, Larabell CA. Putting molecules in their place. *J Cell Biochem*. 2013 Epub ahead of print. 10.1002/jcb.24658
18. Smith EA, Cinquin BP, McDermott G, Le Gros MA, Parkinson DY, Kim HT, Larabell CA. Correlative microscopy methods that maximize specimen fidelity and data completeness, and improve molecular localization capabilities. *J Struct Biol*. 2013; 184:12–20. [PubMed: 23531637]
19. Weiss D, Schneider G, Niemann B, Guttman P, Rudolph D, Schmahl G. Computed tomography of cryogenic biological specimens based on X-ray microscopic images. *Ultramicroscopy*. 2000; 84:185–197. [PubMed: 10945329]
20. Le Gros MA, McDermott G, Uchida M, Knoechel CG, Larabell CA. Highaperture cryogenic light microscopy. *Journal of Microscopy-Oxford*. 2009; 235:1–8.
21. McDermott G, Le Gros MA, Knoechel C, Uchida M, Larabell CA. Soft X-ray tomography and cryogenic light microscopy: The cool combination in cellular imaging. *Trends Cell Biol*. 2009; 19:587–595. [PubMed: 19818625]

22. McDermott G, Fox DM, Epperly L, Wetzler M, Barron AE, Le Gros MA, Larabell CA. Visualizing and quantifying cell phenotype using soft X-ray tomography. *Bioessays*. 2012; 34:320–327. [PubMed: 22290620]
23. McDermott G, Le Gros MA, Larabell CA. Visualizing Cell Architecture and Molecular Location Using Soft X-Ray Tomography and Correlated Cryo-Light Microscopy. *Annual Review of Physical Chemistry*. 2012; 63:225–239. 63.
24. Parkinson DY, Epperly LR, McDermott G, Le Gros MA, Boudreau RM, Larabell CA. Nanoimaging cells using soft x-ray tomography. *Methods Mol Biol*. 2013; 950:457–481. [PubMed: 23086890]
25. Shaner NC, Steinbach PA, Tsien RY. A guide to choosing fluorescent proteins. *Nat Methods*. 2005; 2:905–909. [PubMed: 16299475]
26. Tsien RY. Building and breeding molecules to spy on cells and tumors. *FEBS Lett*. 2005; 579:927–932. [PubMed: 15680976]
27. Giepmans BN, Adams SR, Ellisman MH, Tsien RY. The fluorescent toolbox for assessing protein location and function. *Science*. 2006; 312:217–224. [PubMed: 16614209]
28. Watanabe S, Punge A, Hollopeter G, Willig KI, Hobson RJ, Davis MW, Hell SW, Jorgensen EM. Protein localization in electron micrographs using fluorescence nanoscopy. *Nat Methods*. 2011; 8:80–84. [PubMed: 21102453]
29. Lucic V, Leis A, Baumeister W. Cryo-electron tomography of cells: Connecting structure and function. *Histochem Cell Biol*. 2008; 130:185–196. [PubMed: 18566823]
30. Murphy GE, Narayan K, Lowekamp BC, Hartnell LM, Heymann JAW, Fu J, Subramaniam S. Correlative 3D imaging of whole mammalian cells with light and electron microscopy. *J Struct Biol*. 2011; 176:268–278. [PubMed: 21907806]
31. Sartori A, Gatz R, Beck F, Rigort A, Baumeister W, Plitzko JM. Correlative microscopy: Bridging the gap between fluorescence light microscopy and cryoelectron tomography. *J Struct Biol*. 2007; 160:135–145. [PubMed: 17884579]
32. Schneider G, Guttman P, Rehbein S, Werner S, Follath R. Cryo X-ray microscope with flat sample geometry for correlative fluorescence and nanoscale tomographic imaging. *J Struct Biol*. 2012; 177:212–223. [PubMed: 22273540]
33. Rehbein S, Guttman P, Werner S, Schneider G. Characterization of the resolving power and contrast transfer function of a transmission X-ray microscope with partially coherent illumination. *Opt Express*. 2012; 20:5830–5839. [PubMed: 22418460]
34. Smith EA, Cinquin BP, McDermott G, Le Gros MA, Parkinson DY, Kim HT, Larabell CA. Correlative microscopy methods that maximize specimen fidelity and data completeness, and improve molecular localization capabilities. *J Struct Biol*. 2013
35. Le Gros, MA.; Knoechel, CG.; Uchida, M.; Parkinson, DY.; McDermott, G.; Larabell, CA. Visualizing sub-cellular organization using soft x-ray tomography. In: Engleman, EH., editor. *Comprehensive Biophysics*. Academic Press; Oxford: 2012. p. 90-110.
36. Larabell C, Le Gros M. Whole cell cryo X-ray tomography and protein localization at 50 micron resolution. *Biophys J*. 2004; 86:185A–185A.
37. Baumeister W, Grimm R, Walz J. Electron tomography of molecules and cells. *Trends Cell Biol*. 1999; 9:81–85. [PubMed: 10087625]
38. Kak, AC.; Slaney, M. *Principles of computerized tomographic imaging*. IEEE Press; New York, NY: 1988.
39. Glaeser RM, Taylor KA. Radiation damage relative to transmission electron microscopy of biological specimens at low temperature: a review. *J Microscopy*. 1978; 112:127–138.
40. McEwen BF, Downing KH, Glaeser RM. The relevance of dose-fractionation in tomography of radiation-sensitive specimens. *Ultramicroscopy*. 1995; 60:357–373. [PubMed: 8525549]
41. Niemann B, Rudolph D, Schmahl G. X-ray microscopy with synchrotron radiation. *Appl Opt*. 1976; 15:1883–1884. [PubMed: 20165284]
42. Weiss D. Computed tomography of cryogenic biological specimens based on X-ray microscopic images. *Ultramicroscopy*. 2000; 84:185–197. [PubMed: 10945329]
43. Dubochet J, Adrian M, Chang JJ, Homo JC, Lepault J, McDowell AW, Schultz P. Cryo-electron microscopy of vitrified specimens. *Q Rev Biophys*. 1988; 21:129–228. [PubMed: 3043536]

44. Baumeister W, Vanhecke D, Asano S, Kochovski Z, Fernandez-Busnadiego R, Schrod N, Lucic V. Cryo-electron tomography: methodology, developments and biological applications. *J Microsc.* 2011; 242:221–227. [PubMed: 21175615]
45. Echlin P. Ice crystal damage and radiation effects in relation to microscopy and analysis at low temperatures. *J Microsc.* 1991; 161:159–170. [PubMed: 2016734]
46. Moerner WE, Orrit M. Illuminating single molecules in condensed matter. *Science.* 1999; 283:1670–1676. [PubMed: 10073924]
47. Meyer-Ilse W. High resolution protein localization using soft X-ray microscopy. *J Microsc.* 2001; 201:395–403. [PubMed: 11240856]
48. Heintzmann R, Cremer C. Axial tomographic confocal fluorescence microscopy. *Journal of Microscopy-Oxford.* 2002; 206:7–23.
49. Shapiro D, Thibault P, Beetz T, Elser V, Howells M, Jacobsen C, Kirz J, Lima E, Miao H, Neiman AM, Sayre D. Biological imaging by soft x-ray diffraction microscopy. *Proc Natl Acad Sci U S A.* 2005; 102:15343–15346. [PubMed: 16219701]
50. Miao J, Hodgson KO, Ishikawa T, Larabell CA, LeGros MA, Nishino Y. Imaging whole *Escherichia coli* bacteria by using single-particle x-ray diffraction. *Proc Natl Acad Sci U S A.* 2003; 100:110–112. [PubMed: 12518059]
51. Nelson J, Huang X, Steinbrener J, Shapiro D, Kirz J, Marchesini S, Neiman AM, Turner JJ, Jacobsen C. High-resolution x-ray diffraction microscopy of specifically labeled yeast cells. *Proc Natl Acad Sci U S A.* 2010; 107:7235–7239. [PubMed: 20368463]
52. Huang X, Nelson J, Kirz J, Lima E, Marchesini S, Miao H, Neiman AM, Shapiro D, Steinbrener J, Stewart A, Turner JJ, Jacobsen C. Soft X-ray diffraction microscopy of a frozen hydrated yeast cell. *Phys Rev Lett.* 2009; 103:198101. [PubMed: 20365955]
53. Attwood, DT. *Soft x-rays and extreme ultraviolet radioation: principles and applications.* Cambridge University Press; Cambridge, New York: 1999.
54. Chao W, Harteneck BD, Liddle JA, Anderson EH, Attwood DT. Soft X-ray microscopy at a spatial resolution better than 15 nm. *Nature.* 2005; 435:1210–1213. [PubMed: 15988520]
55. Denbeaux G, Anderson E, Chao W, Eimuller T, Johnson L, Kohler M, Larabell C, Legros M, Fischer P, Pearson A, Schultz G, Yager D, Attwood D. Soft X-ray microscopy to 25 nm with applications to biology and magnetic materials. *Nuclear Instruments & Methods in Physics Research Section a-Accelerators Spectrometers Detectors and Associated Equipment.* 2001; 467:841–844.
56. Falcone R, Jacobsen C, Kirz J, Marchesini S, Shapiro D, Spence J. New directions in X-ray microscopy. *Contemporary Physics.* 2011; 52:293–318.
57. Kirz J, Jacobsen C, Howells M. Soft X-ray microscopes and their biological applications. *Q Rev Biophys.* 1995; 28:33–130. [PubMed: 7676009]
58. Schermelleh L, Carlton PM, Haase S, Shao L, Winoto L, Kner P, Burke B, Cardoso MC, Agard DA, Gustafsson MG, Leonhardt H, Sedat JW. Subdiffraction multicolor imaging of the nuclear periphery with 3D structured illumination microscopy. *Science.* 2008; 320:1332–1336. [PubMed: 18535242]
59. Carlton PM. Three-dimensional structured illumination microscopy and its application to chromosome structure. *Chromosome Res.* 2008; 16:351–365. [PubMed: 18461477]
60. Hertz HM, von Hofsten O, Bertilson M, Vogt U, Holmberg A, Reinspach J, Martz D, Selin M, Christakou AE, Jerlström-Hultqvist J, Svärd S. Laboratory cryo soft X-ray microscopy. *J Struct Biol.* 2012; 177:267–272. [PubMed: 22119891]

Text Box 1**Overview of SXT and FCM****SXT**

- **Spatial Resolution:** The short wavelength of x-rays allows full-field imaging at a spatial resolution of 50 nm or better.
- **Wide-range Specimen Acceptance:** The deep penetration of soft x-ray photons allows fully hydrated cells up to 15 μm thick to be imaged without being sectioned.
- **Unique Image Contrast Mechanism produces Quantitative Images:** Image contrast is obtained directly from the measured attenuation of soft x-rays by the specimen. Illuminating photons are in the 'water window', that is between the K shell absorption edges of carbon (284 eV, $\lambda=4.4$ nm) and oxygen (543 eV, $\lambda=2.4$ nm). Photons within this energy range are absorbed an order of magnitude more strongly by carbon- and nitrogen-containing organic materials than by water.
- **High Data Completeness:** Specimens mounted in thin-walled glass capillaries can be imaged from any angle over 360° of rotation.
- **Specimen Integrity:** Cryo-preserved specimens are robust in terms of radiation damage. As a consequence, sufficient projection images for the calculation of a 3-D tomographic reconstruction can be collected without inducing visible artifacts into the images.

FCM

- **Enhanced Fluorescence Label Working Life at Cryogenic Temperatures:** Fluorescent labels have a significantly increased fluorescence working life at low temperature.
- **Improved Spectral Properties:** The spectral width of the emitted light is typically narrower at cryogenic temperature compared with room temperature.
- **Quantification of Labeled Protein:** Photo-bleaching is less dependent of the local chemical environment in a cryogenic specimen, which means it is possible to quantify the local concentration of a labeled protein more accurately than is possible at room temperature.
- **High Data Completeness:** Fluorescence data can be collected at any arbitrary angle over a full 360° of rotation, allowing collection of otherwise inaccessible data.

Highlights

- We describe a new correlated imaging modality: soft x-ray tomography combined (SXT) with confocal fluorescence tomography (CFT).
- Data from the two modalities are combined accurately and precisely using fiducials visible in both types of data
- Cells imaged by SXT-CFT are maintained close to their native state by cryopreservation.
- SXT-CFT is applicable to most cell types, especially cells grown in suspension.
- ‘Super-resolution’ microscopes being developed for CFT data acquisition match the spatial resolution of SXT.

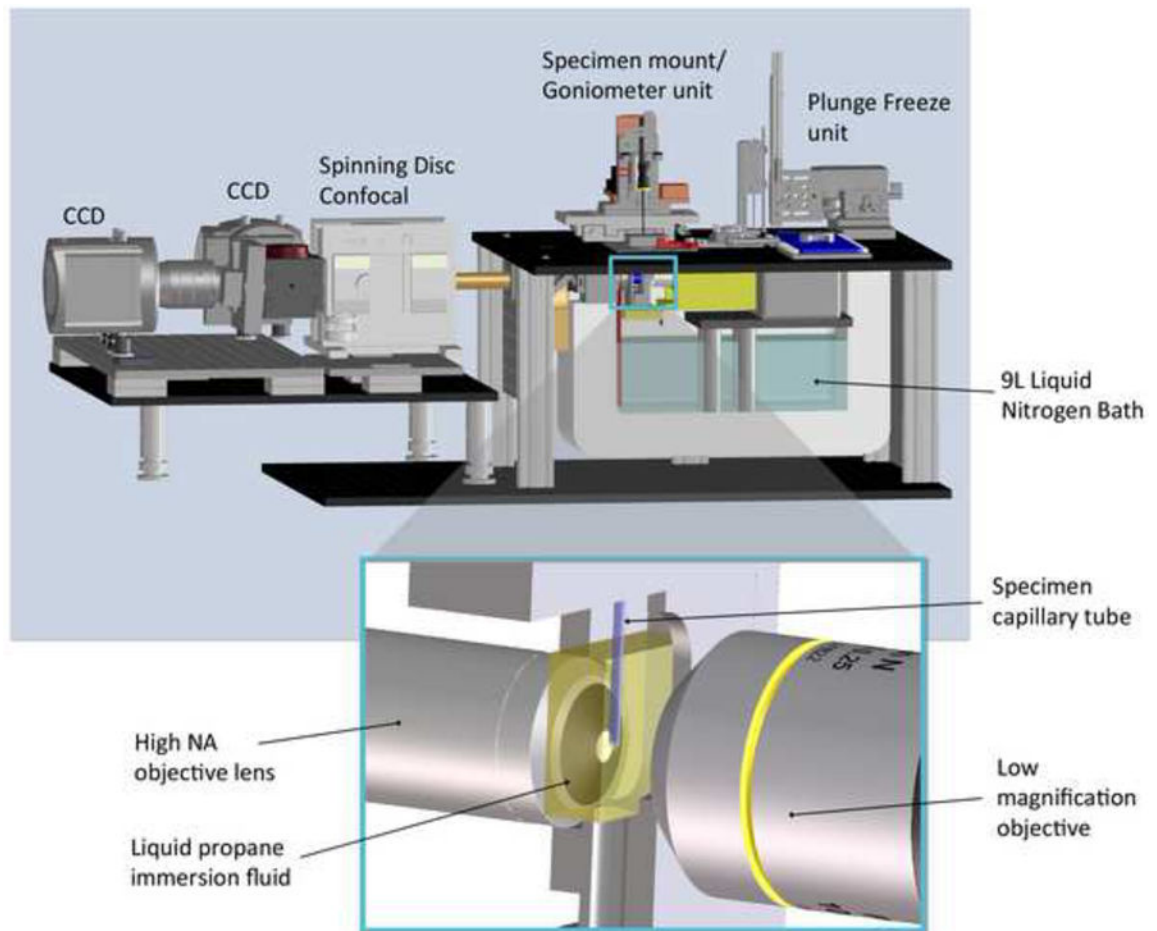


Figure 1. High Numerical Aperture Fluorescence Cryo Microscope (FCM)

Computer-aided design (CAD) of the FCM together with the associated instruments that combine to create a cryogenic imaging workbench. The FCM has two objective lenses and three cameras for high and low-magnification imaging. The high-magnification side images onto Andor EMCCD cameras (red/green channels) using a commercial spinning disk confocal microscope unit. A specimen mount/goniometer mounts thin glass capillaries and permits 360° rotation of the specimen. A 9L liquid Nitrogen bath keeps the microscope stable at ~90°K for several hours without the need for refilling. Specimens are rapidly cryopreserved by rapid plunging into liquid propane using the device mounted to the right hand side of the microscope in this view. The inset shows a magnified view of the high NA (main) objective lens, a specimen capillary tube in an imaging cell filled with liquid propane immersion fluid, and the objective lens for the low-magnification microscope.

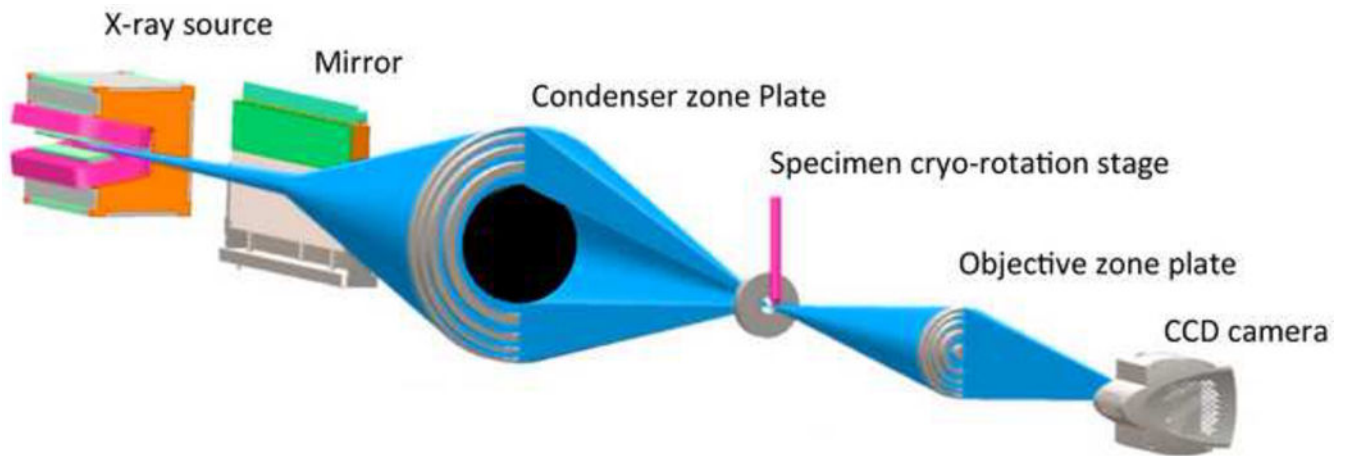


Figure 2. Soft X-ray Microscope: Optical layout together with an example of SXT data
 Schematic representation of XM-2, a soft x-ray microscope located at the Advanced Light Source, Berkeley. A bend magnet (a) in the synchrotron lattice generates an intense swath of soft x-rays. A flat, nickel-coated mirror (b) delivers soft x-rays onto the condenser zone plate (c), which, in combination with the pinhole (d) act as both a monochromator and as a condenser lens to focus the beam onto the specimen mounted in the cryogenic specimen rotation stage. Soft x-rays transmitted by the specimen are focused on to a CCD camera by the objective zone plate (e) onto a CCD camera (f). The optical path taken by the soft x-ray beam is shown in blue.

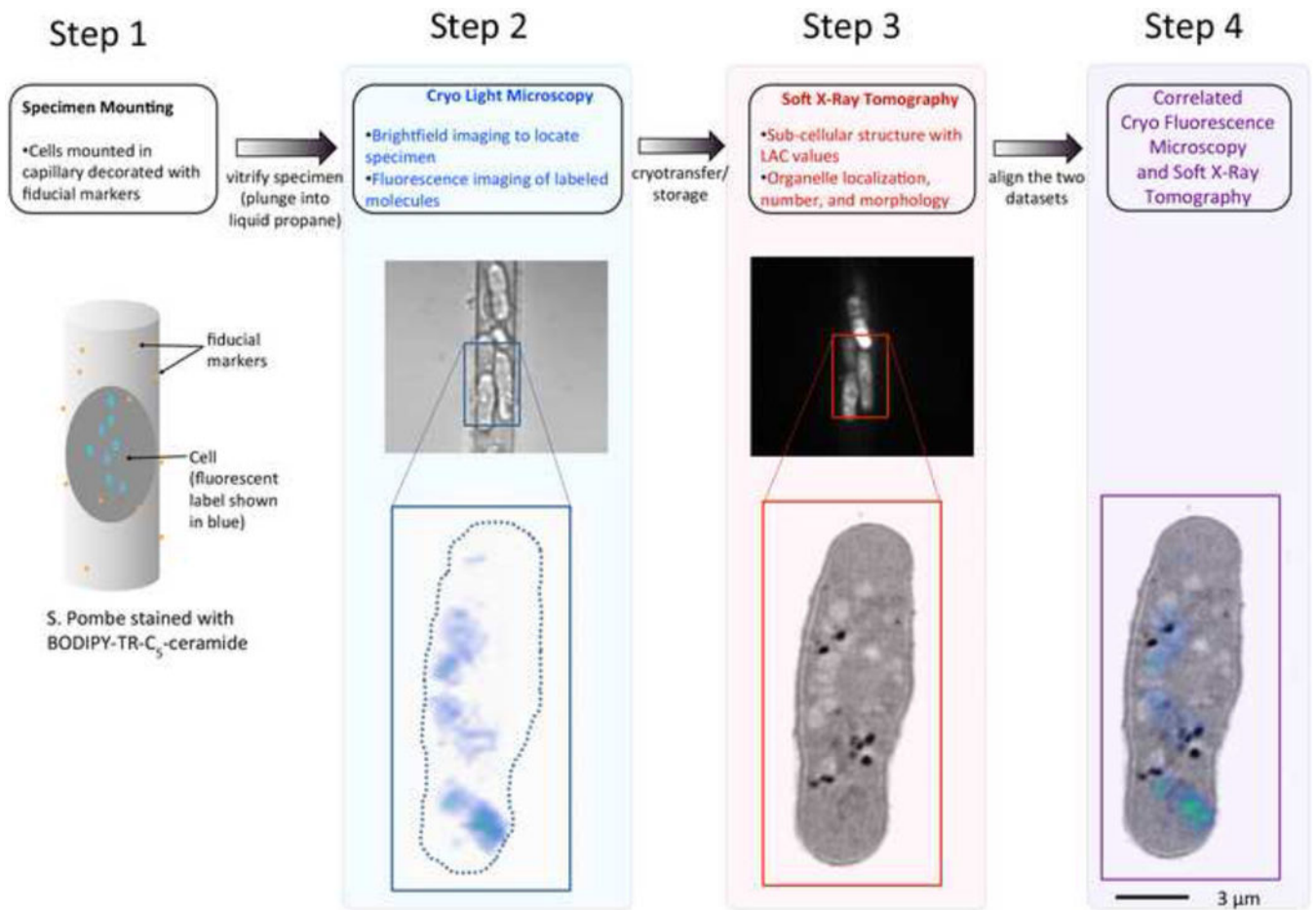


Figure 3. SXT-FCM workflow

Outline of the SXT-FCM workflow. Shown here are *Schizosaccharomyces pombe* cells stained with the vital dye BODIPY-TR-C₅-ceramide, which accumulates in Golgi. **Step 1.** Cells in suspension are pelleted by centrifugation, re-suspended in a small volume of media, and pipetted into thin-walled glass capillaries, the exterior of which have been decorated with fiducial markers (a). **Step 2.** The specimen is vitrified by rapidly plunging the capillary into liquid propane, and then imaged in the FCM (b). **Step 3.** The specimen is then cryo-transferred to the soft x-ray microscope where the specimen is imaged tomographically. The measured contrast is a function of the material's linear absorption coefficient (LAC). **Step 4.** Once the FCM and SXT data sets have been processed they are aligned using the fiducial markers to yield a correlated dataset (d).

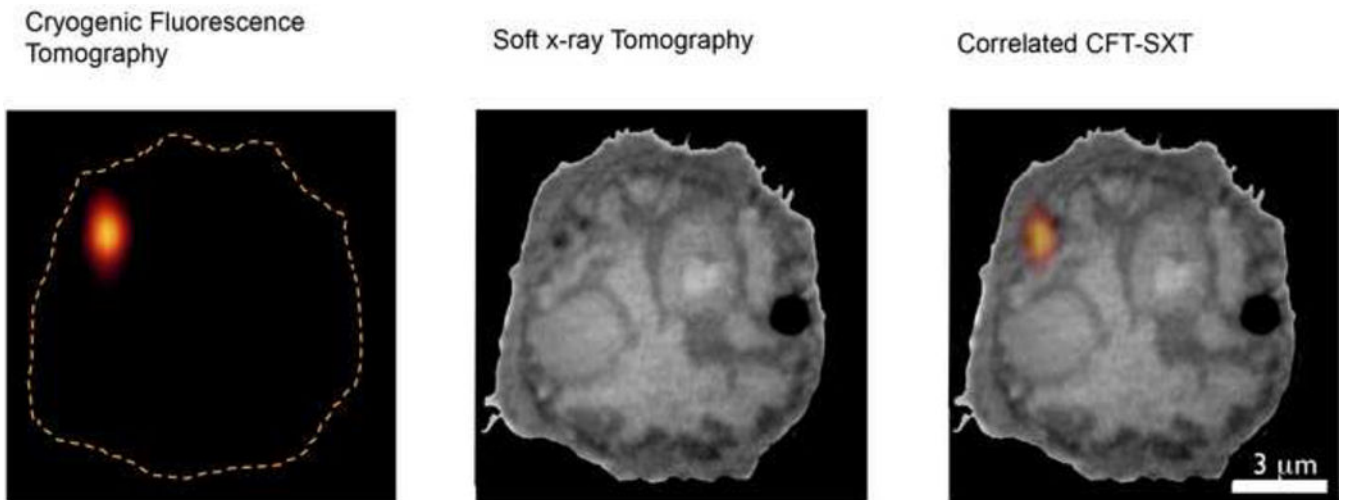


Figure 4. Correlated CFT-SXT imaging of LysoTracker-labeled B Cells

Shown here are mouse B cells that are labeled with the vital dye LysoTracker. Left: A slice from a through-focus FCM dataset, the cell outline is indicated by orange dotted line. Middle: An orthoslice through the SXT reconstruction of the same cell. Right: Overlay of the fluorescence and SXT reconstructions; punctate structures visible in the SXT reconstruction are identified by FCM data as being acidic lysosomes. Scale bar = 3 μ m